

Cite this article as: Chao Rui, Cai Haichao, Li Hang, et al. Effect of Ar/N₂-Ar Co-sputtering Ti Doping on Optical and Mechanical Properties of Ta₂O₅ Coatings[J]. Rare Metal Materials and Engineering, 2024, 53(06): 1574-1581. DOI: 10.12442/j.issn.1002-185X.20230564.

ARTICLE

Effect of Ar/N₂-Ar Co-sputtering Ti Doping on Optical and Mechanical Properties of Ta₂O₅ Coatings

Chao Rui^{1,2,3}, Cai Haichao^{1,2,3}, Li Hang^{1,2}, Lv Wenxue⁴, Xue Yujun^{1,2,3}

¹School of Mechatronics Engineering, Henan University of Science and Technology, Luoyang 471003, China; ²Henan Key Laboratory of Modern Mechanical Design and Transmission System, Luoyang 471003, China; ³Collaborative Innovation Center of Henan Province for High-End Bearing, Luoyang 471003, China; ⁴Laiwu Technician Institute, Laiwu 271100, China

Abstract: In order to explore the effects of Ti doping on the optical and mechanical properties of Ta₂O₅ coatings prepared by Ar/N₂-Ar co-sputtering, Ta₂O₅, N₂-Ta₂O₅, Ti-Ta₂O₅, and N₂-Ti-Ta₂O₅ coatings were prepared on the glass substrate surface by radio frequency and direct current magnetron co-sputtering techniques. The microstructures and surface morphologies of Ta₂O₅, N₂-Ta₂O₅, Ti-Ta₂O₅, and N₂-Ti-Ta₂O₅ coatings were characterized by X-ray diffraction (XRD), scanning electron microscope (SEM), and atomic force microscope (AFM). The optical parameters of the coatings were tested by ultraviolet-visible spectrophotometry. The hardness and Young's modulus of the coatings were tested by nanoindentation. XRD test results show that the Ta₂O₅, N₂-Ta₂O₅, Ti-Ta₂O₅, and N₂-Ti-Ta₂O₅ coatings mainly consist of amorphous phase structure with Ta₂O₅ as the main body. SEM and AFM results show that the coatings deposited on the glass substrate do not have extensive voids. The sputtered particles are uniformly piled and grow on the substrate surface. The coating thicknesses are basically the same and the thickness error is within 5%. The separate introduction of N₂, Ti, and N₂-Ti co-doping can reduce the roughness of Ta₂O₅ coatings. The optical test results show that the separate introduction of N₂ and Ti element can increase the average transmittance of Ta₂O₅ coatings to more than 81%, whereas the average transmittance of N₂-Ti-Ta₂O₅ coatings prepared by N₂-Ti co-doping reduces. Mechanical test results show that compared with that of Ta₂O₅ coating, the hardness of N₂-Ta₂O₅ and N₂-Ti-Ta₂O₅ coatings increases significantly. The hardness of Ti-Ta₂O₅ coatings is basically the same. The elasticity index (H/E) and plasticity index (H^3/E^2) indicate that the N₂-Ta₂O₅ and N₂-Ti-Ta₂O₅ coatings possess better fracture toughness and plastic deformation resistance. The preparation of N₂- and Ti-doped Ta₂O₅ coatings on glass surface can obtain the multifunctional coatings with both excellent optical and mechanical properties, which is represented by N₂-Ta₂O₅ and N₂-Ti-Ta₂O₅ coatings.

Key words: magnetron sputtering; N₂-Ti-Ta₂O₅; coating; optical properties; mechanical properties

Optical coatings are important optical materials with high transparency in the visible range and high reflectivity in the infrared range^[1-2]. The unique characteristics of optical coatings lead to their distinctive types of films among the functional coating materials. With the rapid development of optoelectronic and semiconductor technologies, the demand for high-performance optical films and optical devices is increasing. Therefore, optical coatings and optical devices with superior performance attract much attention in academic research and engineering applications^[3-6]. Metal oxides are ideal candidates for the design and manufacture of protective coatings for optical devices. The most representative Ta-based

oxide has become the research hotspot in various fields^[7-8]. Due to their good optical properties, thermal stability^[9], chemical stability^[10], and high refractive index in the visible and near-infrared region^[11], Ta₂O₅ coatings attract much attention and have been widely used as high-performance materials in the fields of semiconductors, data storage systems, and optical devices^[10,12].

Chen et al^[3] studied the optical properties, such as refractive index, extinction coefficient, thickness, and optical direct and indirect bandgap, of Ta₂O₅ coatings prepared by radio frequency (RF) magnetron sputtering. Bright et al^[13] used reactive magnetron sputtering to deposit Ta₂O₅ coatings with

Received date: September 10, 2023

Foundation item: National Key R&D Program of China (2021YFB3400401)

Corresponding author: Xue Yujun, Ph. D., Professor, School of Mechatronics Engineering, Henan University of Science and Technology, Luoyang 471003, P. R. China, Tel: 0086-379-64278961, E-mail: yjxue@haust.edu.cn

Copyright © 2024, Northwest Institute for Nonferrous Metal Research. Published by Science Press. All rights reserved.

various thicknesses on Si substrates, and determined the optical constants of Ta₂O₅ coatings in a wide spectral range from visible range to far-infrared range. Chen et al^[14] investigated the effect of Ar/O on the properties of Ta₂O₅ coatings as the ion-conducting layers for all-solid-state electrochromic devices. Sertel et al^[15] deposited Ta₂O₅ coatings on Corning glass, Si, GaAs, and Ge substrates by RF magnetron sputtering. The effects of thermal annealing on the structural, optical, and morphological properties of Ta₂O₅ coatings have been investigated and the antireflective properties of the coatings are also widely discussed. Reports show that the coatings deposited on the substrates have uniform distribution of Ta and O elements during the growth process. The optimal transmittance and antireflective properties can be obtained by annealing at 500 °C, and the obtained product can be used as an antireflective layer for optical and photovoltaic applications. In addition to the abovementioned optical properties, Ta₂O₅ has good mechanical properties, such as fine wear resistance and high hardness, which can be used as a protective coating^[16-17]. Ding et al^[18] studied the excellent biocompatibility, high corrosion resistance, and good wear resistance of Ta₂O₅ ceramic coatings. Single- and multi-layer Ta₂O₅ coatings can be prepared on Ti-6Al-4V alloys by magnetron sputtering technique. The microstructure, chemical composition, residual thermal stress, adhesion strength, mechanical properties, tribological behavior, and corrosion resistance of the coatings have been studied. Karbay et al^[19] deposited Ta₂O₅ coating on the glass substrate by sol-gel method. In the ring-to-ring bending test, it is found that the ultimate strength of the glass substrate coated by Ta₂O₅ increases by nearly three times, and the coating shows excellent friction resistance. Generally, the research on Ta₂O₅ coatings mainly focuses on the optical or mechanical properties under specific working conditions. Ta₂O₅ coatings with both excellent optical properties and good mechanical properties are rarely discussed.

In this research, RF and direct current (DC) magnetron co-sputtering techniques were used to investigate the effects of Ar/N₂-Ar co-sputtering Ti doping on the microstructure, optical properties, and mechanical properties of Ta₂O₅ coatings. This research promotes the development of multifunctional coatings with both excellent optical performance parameters and good mechanical properties.

1 Experiment

Ta₂O₅, N₂-Ta₂O₅, Ti-Ta₂O₅, and N₂-Ti-Ta₂O₅ coatings were prepared by JGP045CA multi-target sputtering system. The substrate materials are high transparent quartz glass and N<111>Si wafers. The substrates were ultrasonically cleaned by acetone, anhydrous ethanol, and deionised water for 15 min before deposition, and then dried with high purity N₂ before placement in the sputtering chamber. The vacuum in the sputtering chamber was pumped to 5×10⁻⁴ Pa, and the deposition pressure was 0.8 Pa. Ar gas was the working gas (99.999% purity) with the flow rate of 40 mL/min. N₂ was the mixed gas (99.999% purity) with the flow rate of 20 mL/min.

The target was Ta₂O₅ and metal Ti (99.99% purity), and the distance between the target and the substrate was 80 mm. In order to obtain a clean target surface, the target needs to be pre-sputtered for 10 min by glow discharge. The deposition temperature was room temperature and the deposition duration was 40 min. During the deposition process, the substrate temperature increased due to ion bombardment (<45 °C). Table 1 shows the deposition parameters of Ta₂O₅, N₂-Ta₂O₅, Ti-Ta₂O₅, and N₂-Ti-Ta₂O₅ coatings.

The phase structure and surface morphology of Ta₂O₅, N₂-Ta₂O₅, Ti-Ta₂O₅, and N₂-Ti-Ta₂O₅ coatings were investigated. X-ray diffraction (XRD, XRD-Max2500, Rigaku, Japan) was used to analyze the phase structure of the coatings with different components at the scanning angle of 5° under 50 kV, 150 mA, and Cu Kα radiation. The scanning range was 10°–90°. The surface and cross-section morphologies of the coating were obtained by scanning electron microscope (SEM, Zeiss Sigma 300), and the cross-sectional thickness of the coating was measured. The energy spectrum and element distribution of the coating surface were obtained by energy dispersive spectroscopy (EDS, Smart EDX). The surface morphology of the coating was also studied by atomic force microscope (AFM, Bruker Dimension Icon), and the surface roughness (*R_a*) of the coating was obtained.

The transmission spectrum of the coating was obtained by ultraviolet (UV) -visible spectrophotometer (Shimadzu UV-2700) with the step of 0.5 nm in the wavelength range of 220–850 nm. The optical parameters, such as reflectivity, absorbance, and optical band gap, of the coatings were obtained by spectral inversion fitting. The hardness and elastic modulus of the coatings were obtained by applying the load of 25 mN through nanoindentation tester (ZDT075-07).

2 Results and Discussion

2.1 Coating phase

Fig. 1 shows XRD patterns of Ta₂O₅, N₂-Ta₂O₅, Ti-Ta₂O₅, and N₂-Ti-Ta₂O₅ coatings. It can be seen that the Ta₂O₅, N₂-Ta₂O₅, Ti-Ta₂O₅, and N₂-Ti-Ta₂O₅ coatings show the hill-like diffraction peaks at 2θ=23.81°, 24.37°, 24.59°, and 24.79°, respectively. The coatings mainly exhibit the diffraction peaks of amorphous SiO₂, indicating that the prepared coating sample does not crystallize and has an amorphous structure. The appearance of hill-like diffraction peaks is due to the thinness of the prepared coatings. During XRD scanning, the noise of the glass substrate seriously affects the test results^[20].

Table 1 Deposition parameters and thickness of Ta₂O₅, N₂-Ta₂O₅, Ti-Ta₂O₅, and N₂-Ti-Ta₂O₅ coatings

Sample	Target power/W			Thickness/nm
	Ta ₂ O ₅	Ti	N ₂	
Ta ₂ O ₅	120	-	-	574.6
N ₂ -Ta ₂ O ₅	120	-	20	557.2
Ti-Ta ₂ O ₅	120	60	-	581.3
N ₂ -Ti-Ta ₂ O ₅	120	60	20	561.5

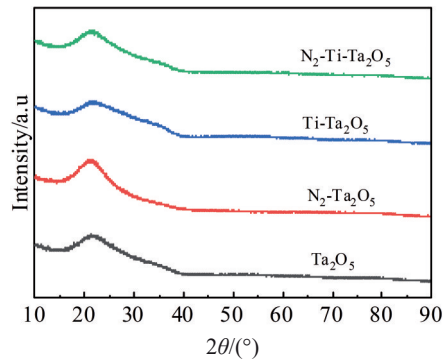


Fig.1 XRD patterns of Ta_2O_5 , $\text{N}_2\text{-Ta}_2\text{O}_5$, $\text{Ti-Ta}_2\text{O}_5$, and $\text{N}_2\text{-Ti-Ta}_2\text{O}_5$ coatings

Because the substrate is not heated or biased during the deposition of coating, the sputtered particles reach the substrate with weak energy and low mobility. The adsorbed atoms can only coalesce in the vicinity of the contacting substrate without dispersing, resulting in the phenomenon that the particles cannot be orderly arranged to form a crystal structure during the deposition process.

2.2 Coating surface morphology

Fig. 2 shows SEM surface and cross-section morphologies of Ta_2O_5 , $\text{N}_2\text{-Ta}_2\text{O}_5$, $\text{Ti-Ta}_2\text{O}_5$, and $\text{N}_2\text{-Ti-Ta}_2\text{O}_5$ coatings. It can be seen that the coatings deposited on the glass substrate do not have large voids. It is inferred that the sputtered particles grow uniformly and are stacked on the substrate surface, but large agglomerated particles appear on all the coating surfaces. This may be because the sputtered particles are not yet evenly spread out after reaching the substrate, and then they are covered by the particles deposited by subsequent sputtering and gradually piled up. Fig. 2e shows the cross-section morphology of Ta_2O_5 coating. It can be seen that the sputtered particles are tightly packed during the coating growth without large cracks. Ta_2O_5 coatings are fully adhered to the substrate. The cross-section morphology of $\text{N}_2\text{-Ta}_2\text{O}_5$ coating (Fig. 2f) shows that the coating deposited in $\text{N}_2\text{-Ar}$ mixed gas atmosphere has irregular cracks during the growth process. The cross-section morphology of $\text{Ti-Ta}_2\text{O}_5$ coating (Fig. 2g) shows that due to the doping of Ti element in the preparation process, the $\text{Ti-Ta}_2\text{O}_5$ coating grows in columnar structure during the deposition process. According to the cross-section morphology of $\text{N}_2\text{-Ti-Ta}_2\text{O}_5$ coating in Fig. 2h, it is found that the columnar structure of $\text{N}_2\text{-Ti-Ta}_2\text{O}_5$ coating becomes blurred, compared with that of $\text{Ti-Ta}_2\text{O}_5$ coating, which is accompanied by the accumulation of particles, but no cracks appear. After Ti doping, the number of agglomerated particles on the coating surface decreases significantly, indicating that the doping of Ti element can improve the surface structure of coatings.

Fig.3 shows 3D-AFM images of Ta_2O_5 , $\text{N}_2\text{-Ta}_2\text{O}_5$, $\text{Ti-Ta}_2\text{O}_5$, and $\text{N}_2\text{-Ti-Ta}_2\text{O}_5$ coatings. The scanning range of the coatings is $3\ \mu\text{m}\times 3\ \mu\text{m}$. It can be seen that although the difference between R_a and root mean square (RMS) value of Ta_2O_5 , $\text{N}_2\text{-}$

Ta_2O_5 , $\text{Ti-Ta}_2\text{O}_5$, and $\text{N}_2\text{-Ti-Ta}_2\text{O}_5$ coatings is obvious, they all remain at the nanometer level. Fig. 3a shows that the Ta_2O_5 coating has the largest R_a and RMS values, which are 1.28 and 1.62 nm, respectively. Through the analysis of Fig.3b and 3c, it is found that Ti element is doped in $\text{N}_2\text{-Ar}$ mixed gas atmosphere. The R_a and RMS values of the $\text{N}_2\text{-Ta}_2\text{O}_5$ coating decrease, which are 0.355 and 0.473, respectively. Similarly, the R_a and RMS values of $\text{Ti-Ta}_2\text{O}_5$ coating also decrease to 1.05 and 1.36 nm, respectively. Fig.3d shows that on the basis of $\text{N}_2\text{-Ta}_2\text{O}_5$ and $\text{Ti-Ta}_2\text{O}_5$ coatings, Ti element is doped after N_2 is introduced. The R_a and RMS values of $\text{N}_2\text{-Ti-Ta}_2\text{O}_5$ coating further reduce to 0.266 and 0.554 nm, respectively. Peaks also appear in the 3D-AFM images of the coatings, which correspond to the appearance of agglomerated particles. Therefore, Ti element is doped in $\text{Ar/N}_2\text{-Ar}$ atmosphere during the preparation of Ta_2O_5 coating. The coating surface becomes smoother, thereby improving the coating flatness, which is beneficial to the optical properties of coatings.

2.3 Optical properties

In order to study the effect of doping elements on the optical properties of Ta_2O_5 coatings, the coating transmittance was measured by UV-visible spectrophotometer in the wavelength range of 220 – 850 nm. Fig. 4 shows the transmittance of Ta_2O_5 , $\text{N}_2\text{-Ta}_2\text{O}_5$, $\text{Ti-Ta}_2\text{O}_5$, and $\text{N}_2\text{-Ti-Ta}_2\text{O}_5$ coatings. In order to eliminate the influence of coating thickness on transmittance, the deposition thickness of the coating is designed as 560 nm. Fig.2 shows that the thickness of Ta_2O_5 , $\text{N}_2\text{-Ta}_2\text{O}_5$, $\text{Ti-Ta}_2\text{O}_5$, and $\text{N}_2\text{-Ti-Ta}_2\text{O}_5$ coatings is approximately 574.6, 557.2, 581.3, and 561.5 nm, respectively, and the thickness error is within 5%. As shown in Fig.4, the transmittance of Ta_2O_5 coating is correlated with the introduction of the doping Ti and N_2 . In the wavelength range of 300–850 nm, it can be observed that all the coatings show high transparency. Intensive deep UV absorption occurs in the UV spectral region (220–300 nm)^[21]. The transmittance of the coatings is gradually increased with the introduction of N_2 and doping Ti. It can be inferred that the transmittance of optical coatings is related to the refractive index, surface roughness, and structural morphology^[22]. The average transmittance of Ta_2O_5 , $\text{N}_2\text{-Ta}_2\text{O}_5$, $\text{Ti-Ta}_2\text{O}_5$, and $\text{N}_2\text{-Ti-Ta}_2\text{O}_5$ coatings at the wavelength of 300–850 nm is 77.25%, 86.33%, 81.46%, and 76.56%, respectively. The average transmittance of $\text{Ti-Ta}_2\text{O}_5$ and $\text{N}_2\text{-Ti-Ta}_2\text{O}_5$ coatings is more than 81%, and the maximum transmittance is more than 93%. The variation of coating transmittance is consistent with the variation of coating roughness. However, the average transmittance of the $\text{N}_2\text{-Ti-Ta}_2\text{O}_5$ coating is abnormally low, which may be related to the increase in the denseness of the surface structure of the coatings. This is because the loose surface structure and small roughness of the coating are beneficial to the light transmission. Table 2 shows the average and maximum transmittance of Ta_2O_5 , $\text{N}_2\text{-Ta}_2\text{O}_5$, $\text{Ti-Ta}_2\text{O}_5$, and $\text{N}_2\text{-Ti-Ta}_2\text{O}_5$ coatings.

Band gap energy (E_g) can directly affect the electronic band structure of materials and the performance of devices, which is an important parameter to characterize semiconductor

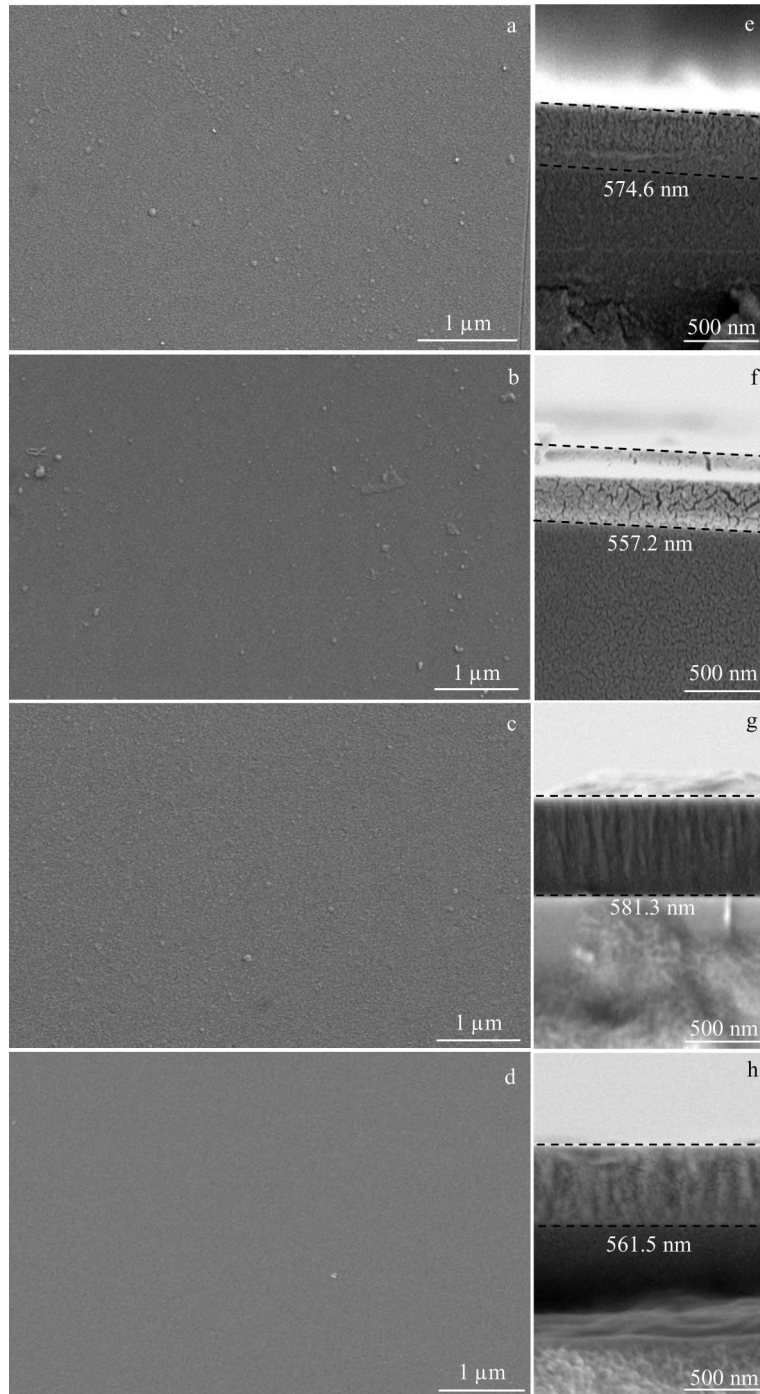


Fig.2 SEM surface (a–d) and cross-section (e–h) morphologies of Ta_2O_5 (a, e), $\text{N}_2\text{-Ta}_2\text{O}_5$ (b, f), $\text{Ti-Ta}_2\text{O}_5$ (c, g), and $\text{N}_2\text{-Ti-Ta}_2\text{O}_5$ (d, h) coatings

materials. In order to evaluate the optical band gap of the coatings, the absorption coefficient (k) of Ta_2O_5 , $\text{N}_2\text{-Ta}_2\text{O}_5$, $\text{Ti-Ta}_2\text{O}_5$, and $\text{N}_2\text{-Ti-Ta}_2\text{O}_5$ coatings was calculated through the transmittance results of the coatings, and the results are shown in Fig.5. Based on the variation of the absorption coefficient as a function of photon energy, the E_g value of the coatings can be obtained by the Tauc relation^[23], as follows:

$$(ahv)^n = C(hv - E_g) \quad (1)$$

$$\alpha = -\ln(T)/d \quad (2)$$

where h is Planck constant, v is the frequency of the incident photon, α is the absorption coefficient, n is a parameter related

to the condition, C is a constant related to the material, d is the thickness of the film, and T is the transmittance of the film. Because Ta_2O_5 is a direct band gap material and the main part of the coatings, Ti is the doping element, and N_2 is the induced gas, $n=2$.

Fig.6 shows the optical band gap energy (E_g) of Ta_2O_5 , $\text{N}_2\text{-Ta}_2\text{O}_5$, $\text{Ti-Ta}_2\text{O}_5$, and $\text{N}_2\text{-Ti-Ta}_2\text{O}_5$ coatings. The optical band gap energy of Ta_2O_5 , $\text{N}_2\text{-Ta}_2\text{O}_5$, $\text{Ti-Ta}_2\text{O}_5$, and $\text{N}_2\text{-Ti-Ta}_2\text{O}_5$ coatings deposited on the glass substrates is 4.45, 4.64, 4.54, and 4.57 eV, respectively. The optical band gap energy of the Ta_2O_5 coating increases slightly after the introduction of N_2

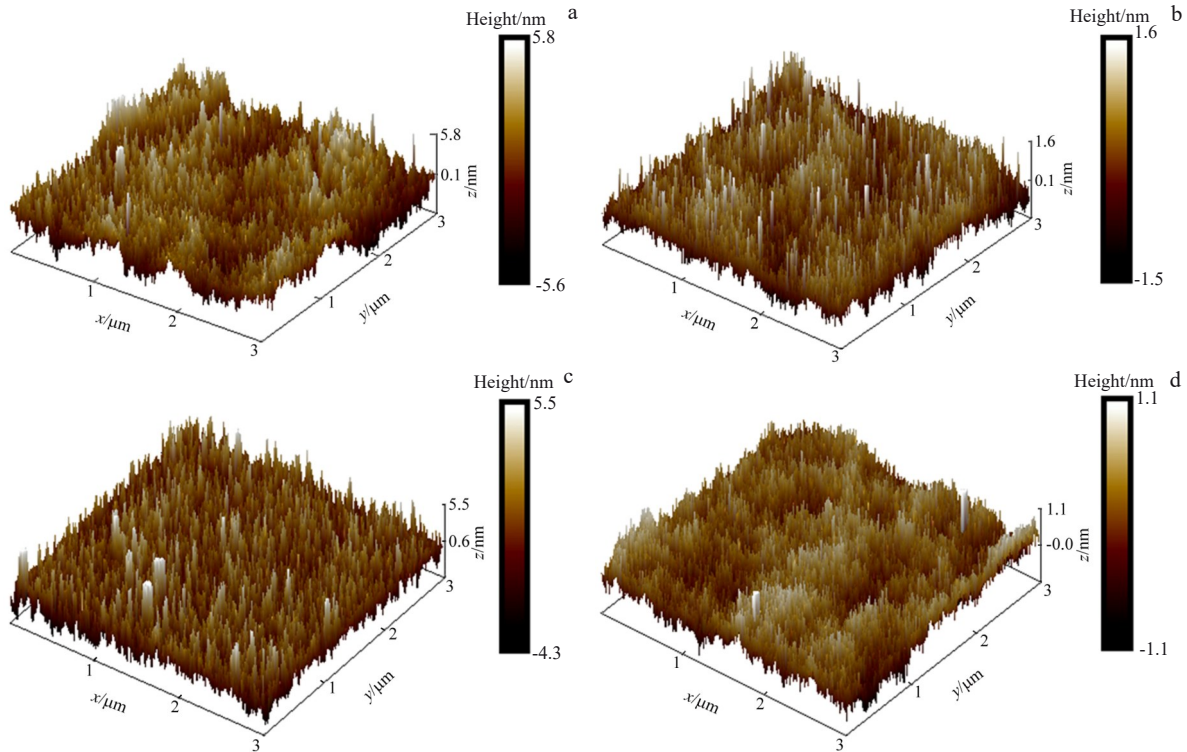


Fig.3 3D-AFM images of Ta₂O₅ (a), N₂-Ta₂O₅ (b), Ti-Ta₂O₅ (c), and N₂-Ti-Ta₂O₅ (d) coatings

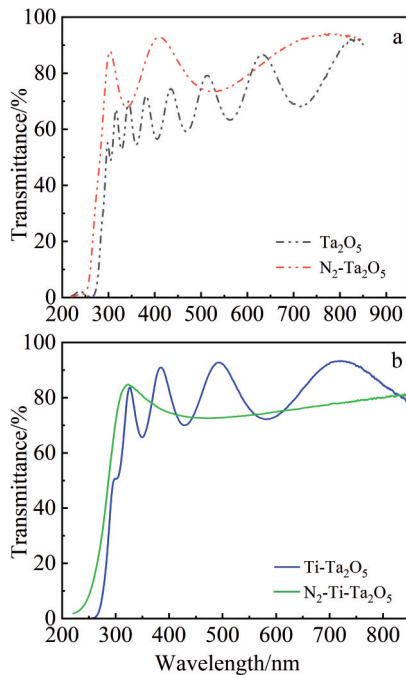


Fig.4 Transmittance of Ta₂O₅ and N₂-Ta₂O₅ coatings (a) as well as Ti-Ta₂O₅ and N₂-Ti-Ta₂O₅ coatings (b)

and Ti element, and the blueshift phenomenon occurs. This phenomenon may be related to the influence of O 1s orbital on the valence band in the host Ta₂O₅ coating. Ta 4f dominates as the conduction band. After the introduction of Ti ions, the Ta₂O₅ oxide is affected by the hybridization of the Ti d orbitals, resulting in a wider band gap spacing.

Table 2 Average transmittance, maximum transmittance, surface roughness R_a , and RMS value of Ta₂O₅, N₂-Ta₂O₅, Ti-Ta₂O₅, and N₂-Ti-Ta₂O₅ coatings

Coating	Average transmittance/%	Maximum transmittance/%	Surface roughness, R_a /nm	RMS/nm
Ta ₂ O ₅	77.25	92.07	1.280	1.620
N ₂ -Ta ₂ O ₅	86.33	93.85	0.355	0.473
Ti-Ta ₂ O ₅	81.46	93.53	1.050	1.360
N ₂ -Ti-Ta ₂ O ₅	76.56	85.18	0.266	0.554

2.4 Mechanical properties

Fig.7 shows the hardness (H), elastic modulus (E), elasticity index (H/E), and plasticity index (H^3/E^2) results of Ta₂O₅, N₂-Ta₂O₅, Ti-Ta₂O₅, and N₂-Ti-Ta₂O₅ coatings. Fig. 7a shows that the hardness of Ta₂O₅, N₂-Ta₂O₅, Ti-Ta₂O₅, and N₂-Ti-Ta₂O₅ coatings is 8.451, 12.371, 8.634, and 12.363 GPa, respectively. The elastic modulus of the coatings is 107.1, 108.3, 151.4, and 173.6 GPa, respectively. The hardness of the coatings increases significantly after the introduction of N₂, and the elastic modulus increases slightly. After doping Ti element, the hardness of the coatings increases slightly, but the elastic modulus increases significantly. The hardness and elastic modulus of the coatings obtained under Ti doping condition in N₂-Ar atmosphere significantly increase, compared with those of Ta₂O₅ coatings. It can be inferred that the N₂-Ti-Ta₂O₅ coating possesses the advantages of both N₂-Ta₂O₅ and Ti-Ta₂O₅ coatings, which may be related to the structural optimization of the coating deposition process.

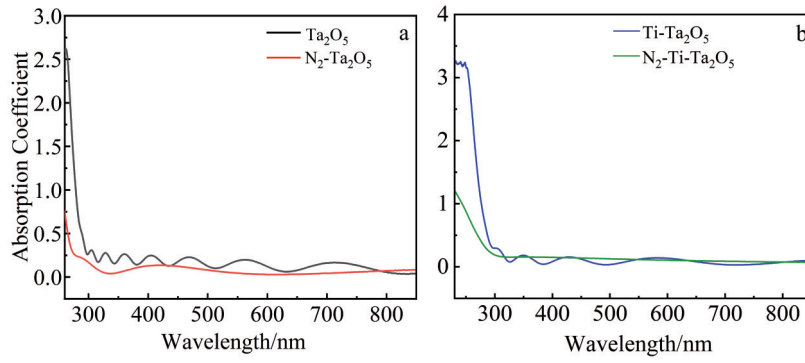


Fig.5 Absorption coefficients of Ta₂O₅ and N₂-Ta₂O₅ coatings (a) as well as Ti-Ta₂O₅ and N₂-Ti-Ta₂O₅ coatings (b)

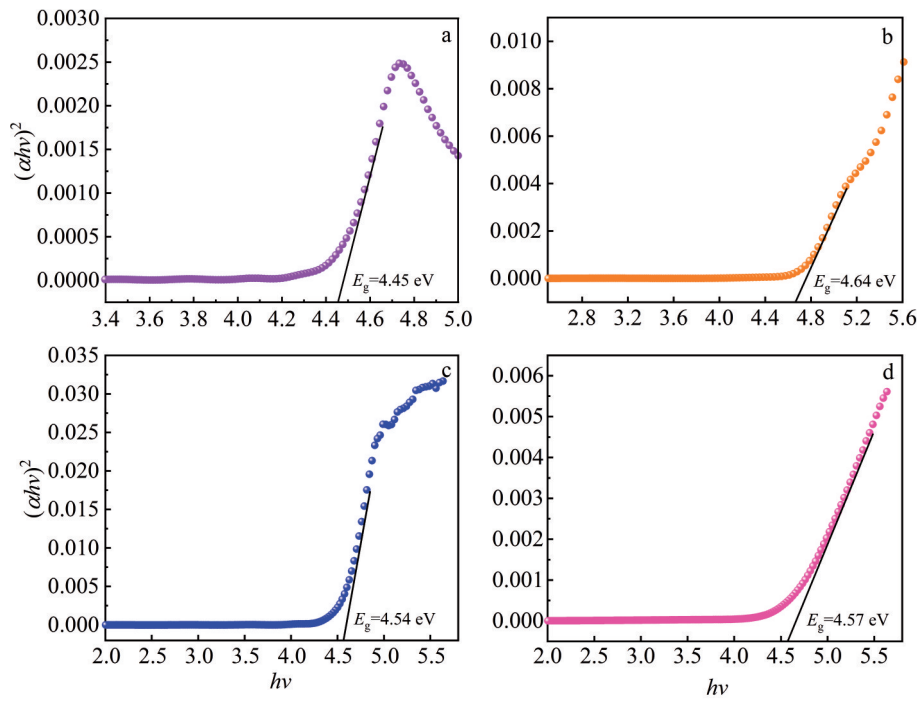


Fig.6 Optical band gap energy curves of Ta₂O₅ (a), N₂-Ta₂O₅ (b), Ti-Ta₂O₅ (c), and N₂-Ti-Ta₂O₅ (d) coatings

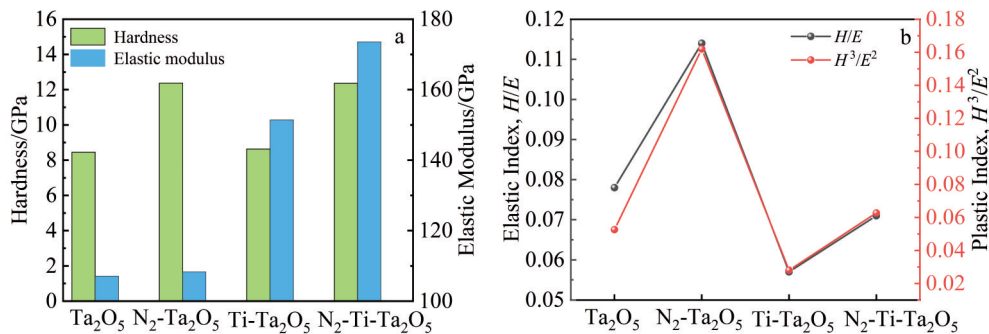


Fig.7 Hardness and elastic modulus (a) as well as elasticity index and plasticity index results (b) of Ta₂O₅, N₂-Ta₂O₅, Ti-Ta₂O₅, and N₂-Ti-Ta₂O₅ coatings

Fig.7b shows the elasticity index (H/E) and plasticity index (H^3/E^2) of Ta₂O₅, N₂-Ta₂O₅, Ti-Ta₂O₅, and N₂-Ti-Ta₂O₅ coatings. The elasticity index is commonly used to evaluate the energy absorption ability through elasticity of material

surface. The higher the elasticity index, the greater the deformation ability under load^[24-25]. The plasticity index expresses the plastic deformation resistance of material, and it is commonly used to simply describe the fracture toughness of

solid coatings^[26]. The higher the H^3/E^2 value, the more difficult the plastic deformation occurring along the shear force direction when the coating is subjected to load. The elasticity indices (H/E) of Ta₂O₅, N₂-Ta₂O₅, Ti-Ta₂O₅, and N₂-Ti-Ta₂O₅ coatings are 0.078, 0.114, 0.057, and 0.071, respectively. The plasticity indices (H^3/E^2) of the coatings are 0.0526, 0.1620, 0.0280, and 0.0627, respectively. The variation trends of H/E and H^3/E^2 are quite different from those of the hardness or elastic modulus of the coatings. The H/E and H^3/E^2 values of the N₂-Ta₂O₅ coating are the largest. On the contrary, the H/E and H^3/E^2 values of Ti-Ta₂O₅ coating are the smallest. For the N₂-Ti-Ta₂O₅ coatings, the values of H/E and H^3/E^2 are between H/E and H^3/E^2 for Ta₂O₅ and N₂-Ta₂O₅ coatings. Compared with N₂-Ta₂O₅ coating, the decrease in H/E and H^3/E^2 values of Ti-Ta₂O₅ coating indicates that the fracture toughness and plastic deformation resistance of the coating are reduced.

3 Conclusions

1) Ta₂O₅, N₂-Ta₂O₅, Ti-Ta₂O₅, and N₂-Ti-Ta₂O₅ coatings all have amorphous phase structure, which mainly consists of Ta₂O₅. With the introduction of N₂ and doping Ti, the agglomerated particles on the coating surface are significantly reduced. The coatings become flat and smooth, and the surface roughness reduces.

2) With the introduction of N₂ and doping Ti, the transmittance of N₂-Ta₂O₅ and Ti-Ta₂O₅ coatings is increased. The average transmittance of N₂-Ta₂O₅ and Ti-Ta₂O₅ coatings is more than 81%, and the maximum transmittance is more than 93%. The average transmittance of N₂-Ti-Ta₂O₅ coating is slightly lower than that of Ta₂O₅ coating. The introduction of N₂ and doping Ti result in the blueshift phenomenon of the coatings and the increase in band gap energy.

3) The hardness of N₂-Ta₂O₅ coating increases significantly, but the elastic modulus is basically the same as that of the Ta₂O₅ coating. The hardness of Ti-Ta₂O₅ coating is basically the same as that of Ta₂O₅ coating, but its elastic modulus increases significantly. The hardness and elastic modulus of N₂-Ti-Ta₂O₅ coating increase obviously. Comparatively, the N₂-Ta₂O₅ coating has better fracture toughness and plastic deformation resistance.

References

- 1 Yang S M, Bin X, Wei Z et al. *Rare Metal Materials and Engineering*[J], 2023, 52(2): 478
- 2 Li K, Xiong Y Q, Wang H et al. *Rare Metal Materials and Engineering*[J], 2022, 51(1): 18
- 3 Chen X Y, Bai R, Huang M D. *Optical Materials*[J], 2019, 97: 109404
- 4 Cakmakci O, Qin Y, Bosel P et al. *Optics Express*[J], 2021, 29(22): 35206
- 5 Sittinger V, Hofer M, Harig T et al. *Surface and Coatings Technology*[J], 2018, 336: 61
- 6 Vlcek J, Belosludtsev A, Rezek J et al. *Surface and Coatings Technology*[J], 2016, 290: 58
- 7 Glynn C, Aureau D, Collins G et al. *Nanoscale*[J], 2015, 7(47): 20227
- 8 Karakawa M, Sugahara T, Hirose Y et al. *Scientific Reports*[J], 2018, 8(1): 10839
- 9 Sekhar M C, Reddy N N K, Akkera H S et al. *Journal of Alloys and Compounds*[J], 2017, 718: 104
- 10 Shang P, Xiong S M, Li L H et al. *Applied Surface Science*[J], 2013, 285: 713
- 11 Ren W, Yang G D, Feng A L et al. *Journal of Advanced Ceramics*[J], 2021, 10(4): 704
- 12 Qiao Z, Pu Y T, Liu H et al. *Thin Solid Films*[J], 2015, 592: 221
- 13 Bright T J, Watjen J I, Zhang Z M et al. *Journal of Applied Physics*[J], 2013, 114(8): 083515
- 14 Chen H C, Jan D J, Lin J H et al. *Solar Energy Materials and Solar Cells*[J], 2019, 203: 110158
- 15 Sertel T, Sonmez N A, Cetin S S et al. *Ceramics International*[J], 2019, 45(1): 11
- 16 Huang H L, Chang Y Y, Chen H J et al. *Journal of Vacuum Science & Technology A*[J], 2014, 32(2): 02B117
- 17 Horandghadim N, Khalil-Allafi J, Urgen M. *Surface & Coatings Technology*[J], 2020, 386: 125458
- 18 Ding Z L, Zhou Q, Wang Y et al. *Ceramics International*[J], 2021, 47(1): 1133
- 19 Karbay I H C, Budakoglu R, Zayim E O. *Applied Surface Science*[J], 2015, 357: 1890
- 20 Huang Tao. *Preparation and Superhydrophilic Mechanism of Porous TiO₂/SiO₂ Composite Films*[D]. Guangzhou: South China University of Technology, 2013 (in Chinese)
- 21 Li C Y, Zhu X P, Zhao W et al. *Acta Photonica Sinica*[J], 2023, 52(6): 126
- 22 Xiang Junhuai, Xu Zhidong, Wang Jun. *Surface Technology*[J], 2023, 52(11): 347 (in Chinese)
- 23 Mandal P, Roy S, Singh U P. *Optical and Quantum Electronics*[J], 2022, 54(8): 476
- 24 Chen X J, Du Y, Chung Y W. *Thin Solid Films*[J], 2019, 688: 137265
- 25 Leyland A, Matthews A. *Wear*[J], 2000, 246(1): 1
- 26 He D Q, Feng Z H, Zheng W W et al. *Journal of Materials Research and Technology*[J], 2023, 25: 6843

Ar/N₂-Ar 共溅射 Ti 掺杂对 Ta₂O₅ 涂层光学和力学性能的影响

晁 瑞^{1,2,3}, 蔡海潮^{1,2,3}, 李 航^{1,2}, 吕文雪⁴, 薛玉君^{1,2,3}

(1. 河南科技大学 机电工程学院, 河南 洛阳 471003)

(2. 河南省机械设计及传动系统重点实验室, 河南 洛阳 471003)

(3. 高端轴承河南省协同创新中心, 河南 洛阳 471003)

(4. 莱芜技师学院, 山东 莱芜 271100)

摘 要: 为了探索 Ar/N₂-Ar 共溅射 Ti 掺杂对 Ta₂O₅ 涂层光学性能和力学性能的影响, 采用射频和直流磁控共溅射技术在玻璃基底表面制备了 Ta₂O₅、N₂-Ta₂O₅、Ti-Ta₂O₅ 和 N₂-Ti-Ta₂O₅ 涂层。利用 X 射线衍射仪 (XRD)、扫描电子显微镜 (SEM)、原子力显微镜 (AFM) 表征了 Ta₂O₅、N₂-Ta₂O₅、Ti-Ta₂O₅ 和 N₂-Ti-Ta₂O₅ 涂层的微观结构和表面形貌; 通过紫外可见分光光度计测试了涂层的光学参数; 采用纳米压痕仪测试了涂层的硬度和杨氏模量。XRD 测试结果表明, Ta₂O₅、N₂-Ta₂O₅、Ti-Ta₂O₅ 和 N₂-Ti-Ta₂O₅ 涂层主要以 Ta₂O₅ 为主体的非晶相结构组成。SEM 和 AFM 结果显示, 沉积在玻璃基底上的涂层未出现大面积空隙, 溅射粒子在基底表面均匀堆积生长, 并且涂层沉积厚度基本一致, 厚度误差在 5% 以内。分别引入 N₂ 和 Ti 及 N₂-Ti 共掺杂, 均可降低 Ta₂O₅ 涂层的粗糙度。光学测试结果表明, 分别引入 N₂ 和 Ti 元素, 可以提高 Ta₂O₅ 涂层的平均透射率至 81% 以上, 而 N₂-Ti 共掺杂制备的 N₂-Ti-Ta₂O₅ 涂层平均透射率降低。力学测试结果显示, 与 Ta₂O₅ 涂层对比, N₂-Ta₂O₅ 和 N₂-Ti-Ta₂O₅ 涂层的硬度显著增大, Ti-Ta₂O₅ 涂层硬度基本一致。弹性指数 (H/E) 和塑性指数 (H^3/E^2) 表明, N₂-Ta₂O₅ 涂层和 N₂-Ti-Ta₂O₅ 涂层具备更好的断裂韧性和抗塑性变形能力。在玻璃表面制备 Ta₂O₅ 掺杂 N₂ 和 Ti 元素的涂层, 可以实现以 N₂-Ta₂O₅ 涂层和 N₂-Ti-Ta₂O₅ 涂层为代表的、同时具备优异光学性能和力学性能的多功能涂层。

关键词: 磁控溅射; N₂-Ti-Ta₂O₅; 涂层; 光学性能; 力学性能

作者简介: 晁 瑞, 男, 1995 年生, 博士生, 河南科技大学机电工程学院, 河南 洛阳 471000, E-mail: chaoruir@163.com